



Published in final edited form as:

Leukemia. 2014 July ; 28(7): 1501–1510. doi:10.1038/leu.2014.32.

The CD37-targeted antibody-drug conjugate IMGN529 is highly active against human CLL and in a novel CD37 transgenic murine leukemia model

Kyle A. Beckwith, B.S.^{1,2}, Frank W. Frizzera, M.S.², Matthew R. Stefanovski, B.S.², William H. Towns, B.S.², Carolyn Cheney, B.S.², Xiaokui Mo, Ph.D.³, Jutta Deckert, Ph.D.⁴, Carlo M. Croce, M.D.⁵, Joseph M. Flynn, M.D.², Leslie A. Andritsos, M.D.², Jeffrey A. Jones, M.D.², Kami J. Maddocks, M.D.², Gerard Lozanski, M.D.⁶, John C. Byrd, M.D.^{2,7,*}, and Natarajan Muthusamy, DVM., Ph.D.^{2,5,*}

¹Medical Scientist Training Program, The Ohio State University, Columbus, OH

²Division of Hematology, Department of Internal Medicine, The Ohio State University, Columbus, OH

³Center for Biostatistics, The Ohio State University, Columbus, OH

⁴ImmunoGen, Inc., Waltham, MA

⁵Department of Molecular Virology, Immunology, and Medical Genetics, The Ohio State University, Columbus, OH

⁶Department of Pathology, The Ohio State University, Columbus OH

⁷Division of Medicinal Chemistry, College of Pharmacy, The Ohio State University, Columbus, OH.

Abstract

Therapeutic regimens for chronic lymphocytic leukemia (CLL) have increasingly utilized monoclonal antibodies since the chimeric anti-CD20 antibody rituximab was introduced. Despite improved clinical outcomes, current CLL therapies are not curative. Therefore, antibodies with greater efficacy and novel targets are desirable. One promising target is CD37, a tetraspanin protein highly expressed on malignant B-cells in CLL and non-Hodgkin lymphoma. While several novel CD37-directed therapeutics are emerging, detailed preclinical evaluation of these agents is

Users may view, print, copy, download and text and data- mine the content in such documents, for the purposes of academic research, subject always to the full Conditions of use: http://www.nature.com/authors/editorial_policies/license.html#terms

Corresponding Author: Natarajan Muthusamy 410 W 12th Ave, Columbus, OH 43210 Phone: (614) 292-8135 Fax: (614) 292-3312 Raj.Muthusamy@osumc.edu.

*J.C.B and N.M. are senior authors and contributed equally to this work.

Authorship

Contribution: K.A.B. planned the research, performed experiments, analyzed data, and wrote the manuscript; F.W.F. generated the hCD37-Tg and identified founder lines; M.R.S. and W.H.T. maintained the mouse colonies and contributed to animal studies; C.C. helped perform some experiments; X.M. performed statistical analysis of data; J.D. provided vital reagents; C.M.C. provided the Eμ-TCL1 mouse; J.M.F, L.A.A., J.A.J., and K.J.M. provided invaluable clinical samples; G.L. contributed reagents, classified clinical cases, reviewed and approved the final manuscript draft; J.C.B and N.M. planned and supervised the research, obtained funding and reagents for the research, analyzed data, reviewed manuscript drafts, and approved the final version of the manuscript.

Conflict of interest: J.D. is an employee of ImmunoGen Inc. The remaining authors have no conflicts of interest to declare.

Supplementary information is available at *Leukemia's* website.

limited by lack of appropriate animal models with spontaneous leukemia expressing the human CD37 (hCD37) target. To address this, we generated a murine CLL model that develops transplantable hCD37+ leukemia. Subsequently, we engrafted healthy mice with this leukemia to evaluate IMG529, a novel hCD37-targeting antibody-drug conjugate. IMG529 rapidly eliminated peripheral blood leukemia and improved overall survival. In contrast, the antibody component of IMG529 could not alter disease course despite exhibiting substantial *in vitro* cytotoxicity. Furthermore, IMG529 is directly cytotoxic to human CLL *in vitro*, depletes B-cells in patient whole blood, and promotes killing by macrophages and NK cells. Our results demonstrate the utility of a novel mouse model for evaluating anti-human CD37 therapeutics and highlight the potential of IMG529 for treatment of CLL and other CD37-positive B-cell malignancies.

Keywords

Chronic Lymphocytic Leukemia; antibody-drug conjugate; CD37

Introduction

Following approval of the anti-CD20 antibody rituximab, use of monoclonal antibodies in cancer therapy has become increasingly common. Rituximab is now a staple of treatment regimens for chronic lymphocytic leukemia (CLL) and non-Hodgkin lymphoma (NHL), demonstrating substantial clinical efficacy when combined with traditional chemotherapeutics.¹⁻³ While anti-CD20 antibodies represent a major advance, relapse is virtually inevitable.⁴ Neoplastic B-cells are not reliant upon CD20 for survival and rituximab resistance is common.⁵ Compounds that target novel surface molecules with defined oncogenic signaling characteristics could enhance our therapeutic armament, synergize with existing treatments, and potentially circumvent resistance. One of the most promising alternative targets is CD37, a tetraspanin protein highly expressed on malignant B-cells in CLL and NHL.^{6,7} While a natural ligand for CD37 remains unknown, signaling induced by the anti-CD37 peptide SMIP-016 has implicated this tetraspanin as a mediator of the PI3K/Akt survival pathway. Through cytoplasmic ITAM and ITIM-like motifs with opposing functions, CD37 can directly participate in both pro-survival and pro-apoptotic signaling by facilitating alterations in the phosphorylation state of Akt.⁸ Furthermore, CD37-deficient mice exhibit impaired generation of plasma cells as a result of defective Akt signaling in germinal center B-cells.⁹

Interest in targeting CD37 has led to the generation of several novel platforms of anti-CD37 therapeutics, including a small modular immunopharmaceutical peptide and an Fc-engineered IgG1 antibody that are currently in clinical trials for CLL.¹⁰⁻¹² This was recently expanded to include IMG529, an antibody-drug conjugate (ADC) in which the cytotoxic maytansine-derivative DM1 is linked to a CD37-targeting humanized IgG1 antibody via a stable SMCC linker.¹³ This strategy seeks to combine the potent cytotoxicity demonstrated by anti-CD37 therapeutics with the specific delivery of DM1, which exerts anti-proliferative effects by disrupting microtubule dynamics during mitosis.¹⁴ The clinical viability of DM1-conjugated antibodies has been demonstrated by ado-trastuzumab emtansine (T-DM1,

KadcylaTM), now approved by the U.S. Food and Drug Administration for treatment of HER2+ metastatic breast cancer.¹⁵ Brentuximab vedotin, which is indicated for the treatment of refractory Hodgkins lymphoma and systemic anaplastic large cell lymphoma, is currently the only other ADC approved for marketing by the FDA.¹⁶ However, given that over 20 ADCs are currently under evaluation in human trials for a wide variety of indications, this therapeutic strategy seems poised to become increasingly prominent.

While CLL was once viewed as a malignancy driven by apoptosis resistance, the importance of a proliferative component and interactions between tumor and the tissue microenvironment has become increasingly apparent.¹⁷⁻²⁰ Current evidence suggests that a subset of transformed B-cells form proliferative centers in lymphoid tissues and are the source of the malignant cells which slowly accumulate in the peripheral blood.²⁰⁻²² *In vivo* measurements indicate that birth rate of CLL B-cells can exceed 1% of the total malignant clone per day.¹⁹ However, it is still unknown whether ADCs carrying anti-mitotic payloads will have utility in CLL given that proliferation is lower than most subtypes of NHL.²³

The *in vivo* preclinical evaluation of antibodies targeting human CD37 (hCD37) has been impeded by the lack of cross-reactivity with mouse CD37. There are no animal models available for evaluating anti-CD37 therapeutics in the context of spontaneous B-cell malignancy, where complex microenvironment interactions in various disease compartments could influence therapeutic efficacy. To address this, we have generated a transgenic mouse which develops hCD37+ B-cell leukemia that is transplantable into syngenic hosts. We then demonstrate the utility of this unique mouse model by using it to evaluate IMGN529 *in vivo*.

Materials and methods

Human samples

Peripheral blood mononuclear cells (PBMCs) were obtained from normal donors or CLL patients in accordance with the Declaration of Helsinki. All subjects gave written, informed consent for their blood products to be used for research under an institutional review board approved protocol. Blood from CLL patients was collected at The Ohio State University Wexner Medical Center (Columbus, OH). Normal cells were obtained from Red Cross partial leukocyte preparations or healthy donor blood. PBMCs were isolated by Ficoll density-gradient centrifugation (Ficoll-Paque Plus, GE Healthcare, Uppsala, Sweden). Except when performing whole blood experiments, all CLL samples underwent negative selection of B-cells with RosetteSep (STEMCELL Technologies, Vancouver, BC, CA) according to manufacturer's protocol. Cells were cultured at 37°C and 5% CO₂ in RPMI 1640 supplemented with 10% heat-inactivated fetal bovine serum (Sigma, St. Louis, MO), 2 mM L-glutamine (Invitrogen, Carlsbad, CA), 56 U/mL penicillin and 56 µg/ml streptomycin (Invitrogen).

Monoclonal antibody therapeutics

Therapeutics used in our studies, which include alemtuzumab, rituximab, ofatumumab, and trastuzumab, were purchased from the pharmacy at The Ohio State University Wexner Medical Center. ImmunoGen, Inc. (Waltham, MA) provided several humanized IgG1

reagents: IMG529, K7153A, and a non-binding chKTI-SMCC-DM1 (IgG-DM1) control ADC.

Mice

The human CD37 transgenic mouse (hCD37-Tg) was generated on a C57BL/6 background at the OSUCCC Transgenic Mouse Facility by conventional methodology we have previously described.²⁴ B-cell restricted hCD37 expression is driven by immunoglobulin (Ig) V_H promoter and Ig_H-μ enhancer elements in the pBH expression vector.²⁴ The transgenic construct was generated by ligating the cDNA sequence of human CD37 (with an additional FLAG sequence) into EcoRI and NotI sites within the pBH vector. To generate our leukemia model, we crossed hemizygous hCD37-Tg mice with homozygous Eμ-TCL1 mice (C57BL/6 background) that have been previously described.^{25,26} Mice were housed in microisolator cages under controlled temperature and humidity. All animal procedures were performed in accordance with Federal and Institutional Animal Care and Use Committee (IACUC) requirements.

Flow cytometry

Flow experiments were performed using Beckman Coulter FC 500 flow cytometers (Brea, CA). Apoptosis assays were conducted on cells stained with fluorescein isothiocyanate (FITC) conjugated Annexin V and propidium iodide (PI) in 1X Annexin V binding buffer (BD Biosciences, San Jose, CA). Other experiments used fluorochrome-labeled monoclonal antibodies against mouse CD3 (17A2), B220 (RA3-6B2), CD19 (ID3), CD5 (53-7.3), CD4 (RM4-5), CD8 (53-6.7), CD45 (30-F11) (BD Biosciences) and anti-human CD37 (K7153A) conjugated to R-Phycoerythrin (K7153A-PE) that was provided by ImmunoGen, Inc. (Waltham, MA). Flow cytometric data was analyzed using Kaluza software (Beckman Coulter), with the exception of cell cycle experiments which were analyzed with Flowjo (Tree Star, Ashland, OR). Gating was verified with appropriate Fluorescence Minus One (FMO) controls. Absolute cell concentrations were obtained by quantitative flow cytometry using Count Bright absolute counting beads (Invitrogen). Quantification of CD37 surface expression was performed using the QuantiBRITE PE bead assay (BD Biosciences) and 1:1 conjugated K7153A-PE.

Mouse leukemia engraftment

Splenocytes from a moribund, leukemic hCD37×TCL1 donor were isolated by Ficoll-Paque density gradient and re-suspended in sterile PBS for injection. Healthy female hCD37-Tg mice received an intravenous lateral tail vein injection of 200 μl containing 1×10⁷ splenocytes. Age-matched mice were randomly assigned to the following treatment groups (n=6-7 per group): the IMG529 ADC, its K7153A antibody component, an IgG-DM1 ADC control, or trastuzumab as an irrelevant humanized IgG1 antibody control. Mice were monitored for disease by flow cytometry on a weekly basis. Upon leukemia diagnosis, a 10 mg/kg dose of the appropriate treatment was administered intraperitoneally and repeat doses were given 2 times per week for 3 weeks (70 mg/kg total). Leukemia onset was defined as when greater than 20% of CD45+ cells in the peripheral blood consisted of CD5+CD19+ leukemic B-cells or when splenomegaly was evident upon light palpation. To avoid

unnecessary suffering, mice were euthanized with CO₂ upon reaching standard IACUC criteria for early removal (e.g. weight loss >20%, severe lethargy, labored breathing).

Direct cytotoxicity assays

Freshly isolated CLL B-cells from patient blood or mouse splenic B-cells were purified using RosetteSep or EasySep kits respectively (STEMCELL Technologies). Cell viability was assessed by Annexin V-FITC and propidium iodide (BD Biosciences) staining after 24 hour incubation at 37°C with 10 µg/ml antibody +/- 50 µg/ml goat anti-human Fc crosslinking antibody (Jackson ImmunoResearch, West Grove, PA). For cell line experiments, Raji cells were incubated with 1 µg/ml antibody for 72 hours. Data are reported as the percentage of remaining viable cells (those that were both Annexin V and PI negative) normalized to untreated control. Samples were analyzed by flow cytometry and at least 20,000 events collected.

Antibody dependent cellular cytotoxicity (ADCC)

The degree of ADCC was assessed using a standard ⁵¹Cr release assay, as described previously.¹⁰ After 30 minutes of treatment with 10 µg/ml antibody, a total of 5×10⁴ CLL target cells labeled with ⁵¹Cr were co-incubated with NK cells obtained from healthy donors for 4 hours at 37°C in 96-well plates at effector-to-target ratios of 25:1, 6.25:1, or without effectors. Following this incubation, supernatants were harvested and chromium release was measured with a Perkin Elmer Wizard 2 gamma counter (Waltham, MA). Maximum chromium release was determined using targets lysed with sodium dodecyl sulfate (SDS). Cytotoxicity was calculated as follows: % Specific lysis = (Experimental ⁵¹Cr release – Spontaneous ⁵¹Cr release) ÷ (Maximum ⁵¹Cr release – Spontaneous ⁵¹Cr release) × 100. NK cells for this assay were enriched from Red Cross partial leukocyte preparations and healthy donor blood using RosetteSep kits (STEMCELL Technologies).

Antibody dependent cellular phagocytosis (ADCP)

Monocytes were isolated from Red Cross partial leukocyte preparations using MACS CD14+ selection kit (Miltenyi Biotec, Auburn, CA) according to manufacturer protocols. Monocytes were cultured in 10 cm² dishes using RPMI 1640/10% FBS containing 20 ng/ml monocyte-colony stimulating factor (M-CSF; R&D Systems, Minneapolis, MN) to promote differentiation into monocyte-derived macrophages (MDMs). Fresh media containing M-CSF was provided every 2 days. After 7-10 days of incubation, adherent macrophages were harvested and labeled with Claret dye (Sigma). CLL cells were labeled with PKH67 fluorescent dye (Sigma), then treated with 10 µg/ml antibody for 1 hour on ice and washed twice. Labeled cells were co-incubated at an effector-to-target ratio of 1:5 (1×10⁶ MDMs and 5×10⁶ CLL cells) for 30 minutes at 37°C. Samples were fixed with 1% paraformaldehyde prior to analysis by flow cytometry. Relative phagocytosis = (% Claret-positive MDMs becoming PKH67+ in the treatment condition) – (% Claret-positive MDMs becoming PKH67+ in the untreated control). At least 10,000 Claret-positive (MDM) events were collected per sample. Gating strategy and representative example data can be found in the supplemental material.

Complement dependent cytotoxicity (CDC)

RosetteSep purified B-cells and plasma were isolated from the blood of CLL patients. In a final volume of 500 μ l, a total of 5×10^5 CLL B-cells were combined with 150 μ l of autologous plasma (+/- heat-inactivation for 30 minutes at 57°C), 10 μ g/ml antibody, and incubated for 1 hour at 37°C. Following this incubation, samples were washed once and dead cells stained with LIVE/DEAD Fixable near-IR (Invitrogen). Cells were then fixed with 1% paraformaldehyde until analysis by flow cytometry. The percentage of lysed cells was calculated by subtracting the percentage of dead cells in the corresponding untreated control. At least 20,000 events were collected per sample.

CLL B-cell depletion in whole blood

Whole blood from CLL patients (90 μ l) was incubated with 10 μ g/ml antibody for 1 hour at 37°C.²⁷ After this treatment, blood was stained with anti-CD3 FITC (UCHT1) and CD19 PE (HIB19) from BD Biosciences. Cal-lyse (Invitrogen) was used to simultaneously lyse RBCs while fixing the leukocytes. Count Bright absolute counting beads were added just prior to analysis by flow cytometry in order to calculate absolute concentrations of cells. To adjust for differences in initial leukemia counts between patients, data was normalized as follows: Percent depletion = $100 \times (1 - [\text{concentration of cells in treated sample}] \div [\text{concentration of cells in untreated control}])$. Additional details are provided in the supplemental materials.

Cell cycle analysis

Raji cells were synchronized with 2 μ g/ml aphidicolin (Sigma) for 24 hours, transferred to fresh media, and treated with 1 μ g/ml antibody for an additional 24 hours. Following incubation, 1×10^6 cells (re-suspended in 1 ml PBS) were fixed by addition of 3 ml absolute ethanol. After fixation for at least 24 hours, these samples were stained in a PBS solution of 0.1% (v/v) Triton X-100, 200 μ g/ml DNase-free RNase, and 30 μ g/ml propidium iodide (Sigma). The proportion of singlet cells in G1, S, and G2 were obtained with Flowjo analysis software (Tree Star) using the Dean-Jett-Fox model and the assumption that the G2 coefficient of variance (CV) is equal to the G1 CV.

In vivo cell proliferation assay

To assess whether IMG529 could inhibit *in vivo* proliferation, we engrafted healthy hCD37-Tg mice with CD37xTCL1 leukemia. After detection of peripheral blood leukemia (Day 0), mice were randomized to groups that would receive either IMG529 or IgG-DM1 control in a blinded fashion. On Day 3 and Day 5 these mice received 10 mg/kg i.p. antibody, followed by 100 μ g ethynyl-2'-deoxyuridine (EdU) on Day 6. Tissues were collected 24 hours later and incorporation of EdU was detected using Click-it EdU Alexa Fluor 647 Flow Cytometry kit (Life Technologies) according to manufacturer recommendations. Gating for EdU positivity was determined using a control mouse which did not receive EdU.

Statistical analysis

For Raji cell line experiments, analysis of variance (ANOVA) was performed. For patient sample data which involved repeated measures, mixed effect models were utilized to account for dependencies across different treatment groups. For the *in vivo* study, log-rank tests were used to compare the survival probabilities between mouse groups. Holm's method was used to adjust multiplicities. SAS 9.3 software was used for data analysis (SAS, Inc; Cary, NC).

Results

The CD37-targeting IMGN529 directly induces apoptosis of CLL B-cells and maintains Fc-dependent killing by innate immune cells *in vitro*

Addressing whether ADCs may be capable of targeting the proliferative component of CLL is complex and ultimately requires a suitable *in vivo* model. However, we initially characterized the antibody-derived activity of the IMGN529 ADC against primary human CLL, which does not proliferate *ex vivo* in the absence of stimulation. Treatment with IMGN529 or its antibody component alone (K7153A) demonstrated significant *in vitro* cytotoxicity against peripheral blood CLL B-cells (Figure 1A and Supplemental Figure S1). This effect was further augmented by the addition of anti-Fc crosslinking antibody, but did not require its presence to induce cellular apoptosis. The ability for these therapies to induce apoptosis of CLL B-cells was not dependent on IgVH mutational status (Supplemental Figure S2). Interestingly, B-cells isolated from healthy donor blood were less susceptible to direct killing by these antibodies (Supplemental Figure S3). IMGN529 and its antibody component K7153A also mediated antibody-dependent cellular cytotoxicity (ADCC) against CLL by healthy donor NK cells (Figure 1B). We observed no significant difference between IMGN529 and K7153A with respect to their ability to mediate ADCC. Furthermore, both agents equally promoted phagocytosis of CLL by monocyte-derived macrophages (Figure 1C and Supplemental Figure S4). Neither K7153A nor IMGN529 exhibited complement-dependent cytotoxicity when CLL B-cells were incubated with autologous plasma (Figure 1D).

While the above experiments are informative, we sought to further evaluate these reagents in a context where the collective impact of multiple potential mechanisms could be appreciated. Therefore, we performed B-cell depletion assays in CLL patient whole blood, where various innate immune components that may contribute to the therapeutic efficacy of antibodies (complement, NK cells, monocytes, and granulocytes) are present in physiologically relevant proportions to leukemia cells. One hour treatment of CLL patient whole blood with IMGN529 or K7153A resulted in significantly greater malignant B-cell depletion than rituximab or alemtuzumab (Figure 1E and Supplemental Figure S5). In addition, CD37-targeted therapeutics avoided the undesirable T-cell depletion that is observed with anti-CD52 alemtuzumab (Figure 1F). A limited analysis suggests that activity in whole blood does not vary on the basis of cytogenetic abnormalities, although a much larger sample size would be required to achieve greater certainty (Supplemental Figure S6). Likewise, IgVH mutational status did not significantly alter activity. (Supplemental Figure S7).

Given the lack of *in vitro* proliferation associated with CLL B-cells, we sought to determine whether delivery of DM1 by IMG529 would have an impact on actively dividing transformed B-cell lines. Raji cells were treated with K7153A, IMG529, or control antibodies for 72 hours. In contrast to what was observed with non-dividing CLL B-cells, IMG529 demonstrated superior cytotoxicity against Raji cells compared to its K7153A antibody component (Figure 2A). Additional testing with the Mec-1 cell line yielded similar results (data not shown). DM1 is known to kill cells through disruption of microtubules, resulting in G2/M arrest and mitotic catastrophe.¹⁴ Consistent with this mechanism, cell cycle analysis of IMG529-treated Raji cells revealed that a substantial proportion were arrested at the G2/M checkpoint (Figure 2B).

Generation of a human CD37 transgenic mouse model of leukemia

It is unknown whether antibody-targeted delivery of anti-mitotic therapies will have benefits in CLL. To evaluate CD37-directed IMG529 in this capacity, we required a model accurately recapitulating the characteristics of human CLL while expressing the human CD37 (hCD37) target protein. As an initial step to address this need, we generated a hCD37 transgenic mouse (hCD37-Tg), which would eventually be crossed with an existing mouse model of CLL. The hCD37-Tg was created using an expression vector that contained IgV_H promoter and Ig_H- μ enhancer elements to achieve B-cell specific hCD37 expression (Figure 3A). Presence of the transgene in founder lines was determined by PCR and copy number by southern blot analysis (Figure 3B and Supplemental Figure S8). B-cell specific hCD37 expression was confirmed by flow cytometry performed on samples from spleen and peripheral blood (Figure 3C-D). These results also demonstrated that hCD37 is not expressed on T-cells in the hCD37-Tg mouse. To determine whether transgenic B-cells were sensitive to anti-CD37 therapeutics *in vitro*, we purified splenic B-cells and incubated them with the anti-CD37 antibody K7153A. This agent demonstrated *in vitro* cytotoxicity against hCD37-Tg B-cells but did not decrease the viability of hCD37-negative B-cells from non-transgenic littermates (Figure 3E-F). The observed cytotoxicity with K7153A prompted us to cross the hCD37-Tg line with the E μ -TCL1 mouse, an established model of IgV_H unmutated CLL which has been extensively characterized as a drug development tool.^{25,26,28-30} B-cells from these hCD37 \times TCL1 offspring retained expression of both transgenes (Figure 4A-B). As expected, elderly mice developed the CD5+CD19+ leukemia previously described in the original E μ -TCL1 mouse.^{25,26} We then confirmed expression of hCD37 on this CD5+CD19+ cell population in the blood, spleen, and lymph nodes of a leukemic hCD37 \times TCL1 animal (Figure 4C).

IMG529 selectively depletes leukemic B-cells *in vivo* and improves overall survival of mice with hCD37 \times TCL1 leukemia

To evaluate the therapeutic potential of IMG529 *in vivo*, we engrafted splenocytes from a leukemic hCD37 \times TCL1 donor into healthy hCD37-Tg recipients and monitored these mice for disease. Upon leukemia development, mice were treated with the IMG529 ADC, its antibody component K7153A, an IgG-DM1 ADC control, or trastuzumab as a non-specific humanized IgG1 control (Figure 5A). In contrast with our *in vitro* cytotoxicity studies using human CLL cells, which showed no significant difference between IMG529 and its antibody component K7153A alone (see Figure 1), improved overall survival was only

observed in mice treated with IMG529 (Figure 5B). One week of IMG529 treatment was sufficient to eliminate peripheral blood leukemia, while the disease continued to progress in other groups (Figure 5C-D). In addition, previously detected splenomegaly disappeared with IMG529 treatment (Supplemental Figure S9). Depletion of hCD37-negative T-cells did not occur with IMG529 (Figure 5E). Only a transient reduction of peripheral CD19+CD5+ B-cells was observed on day 21 after treatment with the K7153A antibody (Figure 5D). To exclude the possibility that transgene overexpression had promoted an exaggerated response to the IMG529, we quantified the hCD37 surface antigen density on transgenic B-cells. This analysis revealed that the protein was expressed at lower levels than in human CLL, suggesting that transgene overexpression could not account for our results (Supplemental Figure S10).

IMG529 eliminates proliferating hCD37×TCL1 leukemia cells *in vivo*

To better characterize the *in vivo* activity of IMG529, we sought to track the effects on the proliferating subset of leukemia cells within lymphoid tissues. Mice were engrafted with hCD37×TCL1 leukemia and randomly assigned to treatment groups upon development of disease (day 0). On days 3 and 5, mice received 10 mg/kg i.p. doses of IMG529 or IgG-DM1 control, followed by EdU injection on day 6 to monitor *in vivo* cell proliferation. At the beginning of the study, the proportions of peripheral blood CD5+CD19+ leukemia were similar, but IMG529 therapy eliminated most leukemia 48 hours after the second dose (Figure 6A). Leukemia cells were present in the blood, spleen, and bone marrow of mice injected with IgG-DM1, but those receiving IMG529 demonstrated significantly less tumor burden in these tissues (Figure 6B-C). By visual inspection, spleens from all mice treated with IMG529 were much smaller than those from control mice. Although it is an underestimate of actual size difference, this is also evident when spleen length is quantified (Figure 6D). Moreover, incorporation of EdU was significantly lower among CD5+CD19+ cells remaining in the spleens of IMG529 treated mice (Figure 6E).

Discussion

Herein we have described the generation of a human CD37 transgenic (hCD37-Tg) and its subsequent cross with the Eμ-TCL1 mouse to develop a model of spontaneous hCD37+ leukemia. This hCD37×TCL1 model addresses the need for improved platforms to preclinically evaluate anti-human CD37 therapeutics. Specifically, it provides the first model of a low-grade B-cell lymphoproliferative disorder that expresses human CD37. We then utilize this model to demonstrate the potent *in vivo* activity of IMG529, which to our knowledge is the first ADC shown to effectively target the proliferative component of CLL *in vivo*.

Existing models for evaluating anti-CD37 therapeutics are limited by their inability to reproduce the full spectrum of disease associated with B-cell malignancies. The most commonly used approach involves xenografts of human cells into immunodeficient mice, but these models fail to demonstrate the same tumor behavior or typical interactions with the tissue microenvironment.³¹ In CLL xenografts the injected cells largely remain in the peritoneal cavity, demonstrating a small presence of leukemic cells in the spleen and bone

marrow while virtually no cells circulate in the peripheral blood.^{32,33} Models of spontaneous leukemia such as the E μ -TCL1 mouse produce a phenotype that more accurately portrays the compartmental distribution seen in human disease.^{25,31} The leukemia developed by the E μ -TCL1 model closely resembles the more aggressive subtype of IgVH unmutated CLL, exhibiting similar behavior, immunodeficiencies, and epigenetic changes as those observed in the human disease.^{25,26,28-30} The major disadvantage of this model, however, is that it cannot be utilized for preclinical evaluation of most therapeutic antibodies as they lack cross-reactivity with the mouse proteins. Expressing the human target protein in transgenic mice is an alternative, as when Heider et al did so to evaluate their Fc-engineered CD37 antibody *in vivo*.¹¹ However, this does not permit evaluation in the context of malignancy, where therapeutic efficacy may be dramatically altered. The hurdle for evaluating anti-CD37 therapies is overcome with the generation of our hCD37 \times TCL1 mouse model. In addition, the hCD37-Tg we used to generate this CLL model could be crossed with other models of spontaneous leukemia/lymphoma for testing CD37 targeted therapeutics in the context of different hematological malignancies.

Our *in vitro* studies of IMG529 show that conjugation of the CD37-targeting K7153A antibody to DM1 does not diminish its ability to promote effector-mediated killing of CLL by NK cells and macrophages. Furthermore, both IMG529 and K7153A greatly surpass rituximab in their ability to deplete malignant B-cells in CLL patient whole blood. We also observed direct cytotoxicity against CLL in the absence of crosslinker, similar to what has been reported with another recently developed anti-CD37 therapeutic (mAb 37.1) but unlike the CD37-directed peptide TRU-016.^{10,11} Interestingly, healthy donor B-cells were less sensitive to anti-CD37 induced apoptosis than human CLL B-cells or splenic B-cells from hCD37-Tg mice. This cannot be explained by decreased expression of the target protein, as normal B-cells do not have less surface CD37.³⁴ Both murine splenic B-cells and human CLL B-cells display high degrees of spontaneous apoptosis during *in vitro* culture. Therefore, observed differences in direct cytotoxicity could be a result of normal human B-cells exhibiting decreased priming to undergo apoptosis, thus reducing their sensitivity to anti-CD37 therapeutics (which are expected to induce expression of pro-apoptotic mitochondrial protein BIM following CD37 ligation).⁸

IMG529 and K7153A were able to mediate cytotoxicity against human CLL cells to the same level in our *in vitro* studies. This is in sharp contrast to what was observed during our *in vivo* studies, where K7153A produced only modest depletion of leukemic B-cells and was unable to significantly alter the disease course in our hCD37 \times TCL1 model. While its antibody alone was not effective, the full IMG529 ADC rapidly eliminated peripheral blood leukemia, reversed splenomegaly and improved overall survival. The different *in vitro* and *in vivo* activity we observed with these agents is not entirely surprising given that CLL cells do not proliferate in culture, which would make the delivery of anti-mitotic DM1 largely irrelevant in these short-term *in vitro* studies. When tested against proliferating Raji cells *in vitro*, IMG529 possessed a distinct advantage over its antibody component with enhanced cytotoxic activity resulting in G2/M cell cycle arrest. We hypothesized that IMG529 eliminated dividing leukemia cells within the proliferative centers via targeted delivery of DM1 *in vivo*, thus resulting in a greater therapeutic benefit than the antibody

alone. This is supported by the observation that peripheral leukemia depletion with IMG529 was accompanied by a rapid decrease in splenomegaly. To further investigate the *in vivo* activity of IMG529, we monitored its effects on leukemia cells within various compartments of disease and examined those from lymphoid tissues for signs of proliferation using EdU. In doing so, we demonstrated that IMG529 is effective at targeting leukemia in both peripheral blood and the lymphoid compartment. EdU incorporation was largely absent among the few CD5+CD19+ cells that remained after 2 doses, suggesting that IMG529 was indeed eliminating this proliferative subset of cells. Additionally, the splenomegaly observed with IgG-DM1 controls was not present in mice receiving IMG529. While a small number of leukemia cells remained after 2 doses, it is evident that IMG529 is highly active across multiple compartments of disease in this CLL mouse model. Given that the expression of hCD37 was suboptimal compared to human CLL, it is unlikely that antigen density has led to an exaggerated response in the mouse model. For this reason, delivery of the cytotoxic DM1 payload is likely even more efficient on human CLL cells.

As clinical study of IMG529 moves forward, it would be worthwhile to explore potential combination therapies that may take advantage of the unique therapeutic properties of this ADC. Given that IMG529 maintains the Fc-mediated effector functions of the antibody from which it was generated, combination with immunomodulatory drugs (such as lenalidomide) could prove effective. The anti-CD37 peptide TRU-016 previously demonstrated *in vitro* synergy with PI3K inhibitors.⁸ Therefore, it may also be worthwhile to explore combinations with inhibitors of PI3K δ such as GS-1101 and IPI-145, which are both currently under evaluation in Phase III clinical trials for CLL. The newly generated hCD37 \times TCL1 mouse model provides a unique tool that will enable the evaluation of combination strategies for IMG529 and other CD37-targeted therapeutics in an immunocompetent model of spontaneous CLL.

To summarize, we have generated a mouse model which develops a transplantable CD5+CD19+hCD37+ leukemia and demonstrated its utility for the evaluation of anti-CD37 therapeutics. This model facilitated improved preclinical studies of IMG529, elucidating its robust anti-leukemic effects *in vivo*. This is impressive in the context of the E μ -TCL1 leukemia that is somewhat resistant to treatment.^{26,35,36} Given the significant benefits we observed with IMG529, despite relatively low hCD37 expression, we propose that this therapeutic could exhibit efficacy in a wide range of CD37-positive human B-cell malignancies.

Supplementary Material

Refer to Web version on PubMed Central for supplementary material.

Acknowledgements

This work was supported by the the National Cancer Institute (7P01CA095426-09 and 1R01CA159296-01A1), Leukemia and Lymphoma Society (LLS 7080-06 / 7004-11), Michael and Judy Thomas, Harry Mangurian Foundation, and the D. Warren Brown Foundation. K.A.B. received additional support from a Pelotonia fellowship.

References

1. Byrd JC, Rai K, Peterson BL, Appelbaum FR, Morrison VA, Kolitz JE, et al. Addition of rituximab to fludarabine may prolong progression-free survival and overall survival in patients with previously untreated chronic lymphocytic leukemia: an updated retrospective comparative analysis of CALGB 9712 and CALGB 9011. *Blood*. 2005; 105(1):49–53. [PubMed: 15138165]
2. Badoux XC, Keating MJ, Wang X, O'Brien SM, Ferrajoli A, Faderl S, et al. Fludarabine, cyclophosphamide, and rituximab chemoimmunotherapy is highly effective treatment for relapsed patients with CLL. *Blood*. 2011; 117(11):3016–24. [PubMed: 21245487]
3. Plosker GL, Figgitt DP. Rituximab: a review of its use in non-Hodgkin's lymphoma and chronic lymphocytic leukaemia. *Drugs*. 2003; 63(8):803–43. [PubMed: 12662126]
4. Woyach JA, Ruppert AS, Heerema NA, Peterson BL, Gribben JG, Morrison VA, et al. Chemoimmunotherapy with fludarabine and rituximab produces extended overall survival and progression-free survival in chronic lymphocytic leukemia: long-term follow-up of CALGB study 9712. *J Clin Oncol*. 2011; 29(10):1349–55. [PubMed: 21321292]
5. Rezvani AR, Maloney DG. Rituximab resistance. *Best Pract Res Clin Haematol*. 2011; 24(2):203–16. [PubMed: 21658619]
6. Link MP, Bindl J, Meeker TC, Carswell C, Doss CA, Warnke RA, et al. A unique antigen on mature B cells defined by a monoclonal antibody. *J Immunol*. 1986; 137(9):3013–8. [PubMed: 3489782]
7. Schwartz-Albiez R, Dorken B, Hofmann W, Moldenhauer G. The B cell-associated CD37 antigen (gp40-52). Structure and subcellular expression of an extensively glycosylated glycoprotein. *J Immunol*. 1988; 140(3):905–14.
8. Lapalombella R, Yeh YY, Wang L, Ramanunni A, Rafiq S, Jha S, et al. Tetraspanin CD37 directly mediates transduction of survival and apoptotic signals. *Cancer Cell*. 2012; 21(5):694–708. [PubMed: 22624718]
9. van Spriel AB, de Keijzer S, van der Schaaf A, Gartlan KH, Sofi M, Light A, et al. The tetraspanin CD37 orchestrates the alpha(4)beta(1) integrin-Akt signaling axis and supports long-lived plasma cell survival. *Sci Signal*. 2012; 5(250):ra82. [PubMed: 23150881]
10. Zhao X, Lapalombella R, Joshi T, Cheney C, Gowda A, Hayden-Ledbetter MS, et al. Targeting CD37-positive lymphoid malignancies with a novel engineered small modular immunopharmaceutical. *Blood*. 2007; 110(7):2569–77. [PubMed: 17440052]
11. Heider KH, Kiefer K, Zenz T, Volden M, Stilgenbauer S, Ostermann E, et al. A novel Fc-engineered monoclonal antibody to CD37 with enhanced ADCC and high proapoptotic activity for treatment of B-cell malignancies. *Blood*. 2011; 118(15):4159–68. [PubMed: 21795744]
12. Krause G, Patz M, Isaeva P, Wigger M, Baki I, Vondey V, et al. Action of novel CD37 antibodies on chronic lymphocytic leukemia cells. *Leukemia*. 2012; 26(3):546–9. [PubMed: 21886169]
13. Deckert J, Park PU, Chicklas S, Yi Y, Li M, Lai KC, et al. A novel anti-CD37 antibody-drug conjugate with multiple anti-tumor mechanisms for the treatment of B-cell malignancies. *Blood*. 2013; 122(20):3500–10. [PubMed: 24002446]
14. Oroudjev E, Lopus M, Wilson L, Audette C, Provenzano C, Erickson H, et al. Maytansinoid-antibody conjugates induce mitotic arrest by suppressing microtubule dynamic instability. *Mol Cancer Ther*. 2010; 9(10):2700–13. [PubMed: 20937595]
15. Verma S, Miles D, Gianni L, Krop IE, Welslau M, Baselga J, et al. Trastuzumab emtansine for HER2-positive advanced breast cancer. *N Engl J Med*. 2012; 367(19):1783–91. [PubMed: 23020162]
16. de Claro RA, McGinn K, Kwitkowski V, Bullock J, Khandelwal A, Habtemariam B, et al. U.S. Food and Drug Administration approval summary: brentuximab vedotin for the treatment of relapsed Hodgkin lymphoma or relapsed systemic anaplastic large-cell lymphoma. *Clin Cancer Res*. 2012; 18(21):5845–9. [PubMed: 22962441]
17. Messmer BT, Messmer D, Allen SL, Kolitz JE, Kudalkar P, Cesar D, et al. In vivo measurements document the dynamic cellular kinetics of chronic lymphocytic leukemia B cells. *J Clin Invest*. 2005; 115(3):755–64. [PubMed: 15711642]
18. Chiorazzi N. Cell proliferation and death: forgotten features of chronic lymphocytic leukemia B cells. *Best Pract Res Clin Haematol*. 2007; 20(3):399–413. [PubMed: 17707829]

19. Caligaris-Cappio F. Role of the microenvironment in chronic lymphocytic leukaemia. *Br J Haematol.* 2003; 123(3):380–8. [PubMed: 14616995]
20. Soma LA, Craig FE, Swerdlow SH. The proliferation center microenvironment and prognostic markers in chronic lymphocytic leukemia/small lymphocytic lymphoma. *Hum Pathol.* 2006; 37(2): 152–9. [PubMed: 16426914]
21. Caligaris-Cappio F, Ghia P. Novel insights in chronic lymphocytic leukemia: are we getting closer to understanding the pathogenesis of the disease? *J Clin Oncol.* 2008; 26(27):4497–503. [PubMed: 18662968]
22. Vandewoestyne ML, Pede VC, Lambein KY, Dhaenens MF, Offner FC, Praet MM, et al. Laser microdissection for the assessment of the clonal relationship between chronic lymphocytic leukemia/small lymphocytic lymphoma and proliferating B cells within lymph node pseudofollicles. *Leukemia.* 2011; 25(5):883–8. [PubMed: 21321570]
23. Broyde A, Boycov O, Strenov Y, Okon E, Shpilberg O, Bairey O. Role and prognostic significance of the Ki-67 index in non-Hodgkin's lymphoma. *Am J Hematol.* 2009; 84(6):338–43. [PubMed: 19384938]
24. Chen HC, Byrd JC, Muthusamy N. Differential role for cyclic AMP response element binding protein-1 in multiple stages of B cell development, differentiation, and survival. *J Immunol.* 2006; 176(4):2208–18. [PubMed: 16455977]
25. Bichi R, Shinton SA, Martin ES, Koval A, Calin GA, Cesari R, et al. Human chronic lymphocytic leukemia modeled in mouse by targeted TCL1 expression. *Proc Natl Acad Sci U S A.* 2002; 99(10):6955–60. [PubMed: 12011454]
26. Johnson AJ, Lucas DM, Muthusamy N, Smith LL, Edwards RB, De Lay MD, et al. Characterization of the TCL-1 transgenic mouse as a preclinical drug development tool for human chronic lymphocytic leukemia. *Blood.* 2006; 108(4):1334–8. [PubMed: 16670263]
27. Vugmeyster Y, Howell K, Bakshl A, Flores C, Canova-Davis E. Effect of anti-CD20 monoclonal antibody, Rituxan, on cynomolgus monkey and human B cells in a whole blood matrix. *Cytometry A.* 2003; 52(2):101–9. [PubMed: 12655653]
28. Yan XJ, Albesiano E, Zanasi N, Yancopoulos S, Sawyer A, Romano E, et al. B cell receptors in TCL1 transgenic mice resemble those of aggressive, treatment-resistant human chronic lymphocytic leukemia. *Proc Natl Acad Sci U S A.* 2006; 103(31):11713–8. [PubMed: 16864779]
29. Ramsay AG, Johnson AJ, Lee AM, Gorgun G, Le Dieu R, Blum W, et al. Chronic lymphocytic leukemia T cells show impaired immunological synapse formation that can be reversed with an immunomodulating drug. *J Clin Invest.* 2008; 118(7):2427–37. [PubMed: 18551193]
30. Chen SS, Raval A, Johnson AJ, Hertlein E, Liu TH, Jin VX, et al. Epigenetic changes during disease progression in a murine model of human chronic lymphocytic leukemia. *Proc Natl Acad Sci U S A.* 2009; 106(32):13433–8. [PubMed: 19666576]
31. Macor P, Secco E, Zorzet S, Tripodo C, Celeghini C, Tedesco F. An update on the xenograft and mouse models suitable for investigating new therapeutic compounds for the treatment of B-cell malignancies. *Curr Pharm Des.* 2008; 14(21):2023–39. [PubMed: 18691113]
32. Shimoni A, Marcus H, Canaan A, Ergas D, David M, Berrebi A, et al. A model for human B-chronic lymphocytic leukemia in human/mouse radiation chimera: evidence for tumor-mediated suppression of antibody production in low-stage disease. *Blood.* 1997; 89(6):2210–8. [PubMed: 9058746]
33. Durig J, Ebeling P, Grabellus F, Sorg UR, Mollmann M, Schutt P, et al. A novel nonobese diabetic/severe combined immunodeficient xenograft model for chronic lymphocytic leukemia reflects important clinical characteristics of the disease. *Cancer Res.* 2007; 67(18):8653–61. [PubMed: 17875705]
34. Barrena S, Almeida J, Yunta M, Lopez A, Fernandez-Mosteirin N, Giralt M, et al. Aberrant expression of tetraspanin molecules in B-cell chronic lymphoproliferative disorders and its correlation with normal B-cell maturation. *Leukemia.* 2005; 19:1376–83. [PubMed: 15931266]
35. Lucas DM, Edwards RB, Lozanski G, West DA, Shin JD, Vargo MA, et al. The novel plant-derived agent silvestrol has B-cell selective activity in chronic lymphocytic leukemia and acute lymphoblastic leukemia in vitro and in vivo. *Blood.* 2009; 113(19):4656–66. [PubMed: 19190247]

36. Lapalombella R, Sun Q, Williams K, Tangeman L, Jha S, Zhong Y, et al. Selective inhibitors of nuclear export show that CRM1/XPO1 is a target in chronic lymphocytic leukemia. *Blood*. 2012; 120(23):4621–34. [PubMed: 23034282]

Author Manuscript

Author Manuscript

Author Manuscript

Author Manuscript

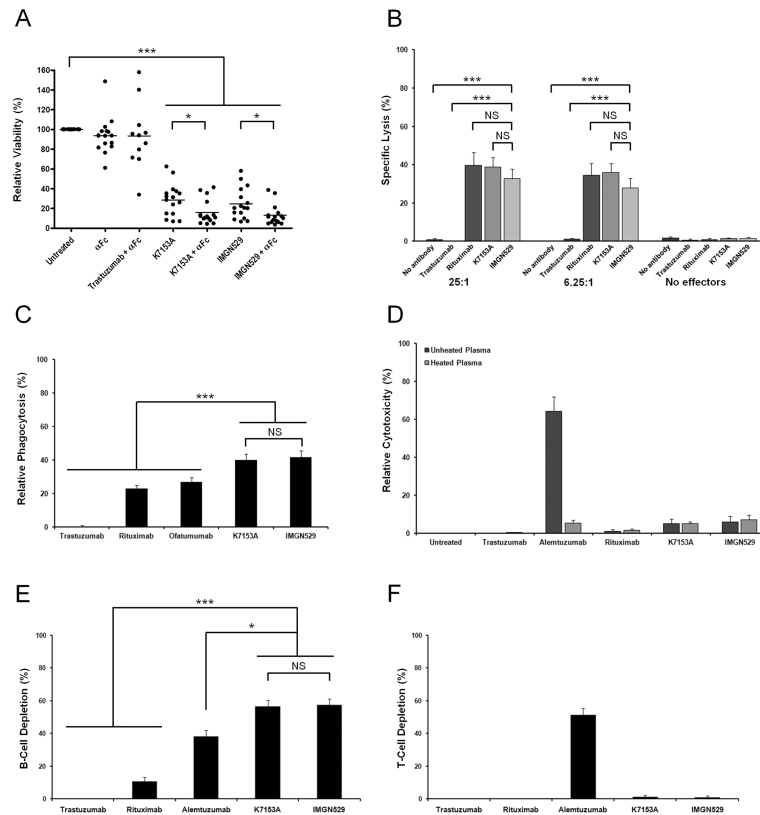


Figure 1. The anti-CD37 antibody-drug conjugate IMGN529 demonstrates *in vitro* activity against neoplastic B-cells from human CLL patients

(A) Viability of freshly isolated CLL patient B-cells (n=16) following 24 hour treatment with 10 μ g/ml IMGN529 or its antibody component K7153A +/- 50 μ g/ml crosslinking antibody (α Fc). Anti-HER2/neu antibody trastuzumab included as an additional negative control for n=11 patients. Data are normalized to untreated controls. Significance is indicated by asterisks (*p<0.05, ***p<0.0001, or NS if p>0.05). (B) NK cell mediated antibody-dependent cytotoxicity as measured by 51 Cr release assay. CLL target cells (n=7) were incubated with 10 μ g/ml antibody for 30 minutes, followed by incubation with healthy donor NK cells (n=8) for 4 hours. Mean specific lysis displayed for n=18 NK/CLL combinations with error bars indicating standard error of the mean (SEM). (C) Induced phagocytosis of CLL cells by monocyte-derived macrophages (MDMs) following 1 hour incubation with 10 μ g/ml antibody. Relative phagocytosis displayed for a total of n=10 MDM/CLL combinations (7 MDMs, 5 CLL) with error bars indicating SEM. (D) Complement-dependent cytotoxicity assay for B-CLL incubated with 10 μ g/ml antibody and autologous plasma (+/- heat inactivation) for 1 hour. Mean values displayed for n=9 CLL patients with error bars indicating SEM. (E,F) CLL patient whole blood was treated with 10 μ g/ml antibody for 1 hour at 37°C. B-cells and T-cells were stained with anti-CD19 and CD3 antibodies respectively. Counts were obtained using CountBright absolute counting beads and normalized to untreated control. Mean percent depletion of B-cells (E) and T-cells

(F) are displayed for n=23 CLL patients with error bars indicating SEM. Greater than 97% of the CD19+ cells in these patients were confirmed to be malignant CD5+ B-cells.

Author Manuscript

Author Manuscript

Author Manuscript

Author Manuscript

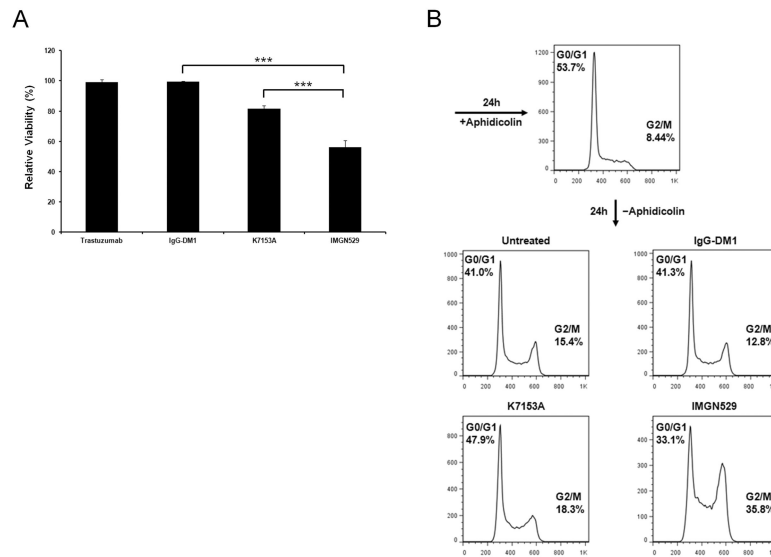


Figure 2. IMGN529 exhibits superior cytotoxicity compared to K7153A and induces mitotic arrest in a proliferating B-cell line *in vitro*

(A) Raji cells were treated with 1 $\mu\text{g/ml}$ K7153A, IMGN529, or relevant controls for 72 hours and viability assayed by Annexin V and propidium iodide staining. Data are normalized to untreated control and reported as mean with error bars indicating SEM for $n=5$ replicate cultures from two independent experiments. (B) Cell cycle analysis of Raji cells that were synchronized with the DNA polymerase inhibitor aphidicolin for 24 hours, released from this inhibition, and then treated with 1 $\mu\text{g/ml}$ antibody for 24 hours.

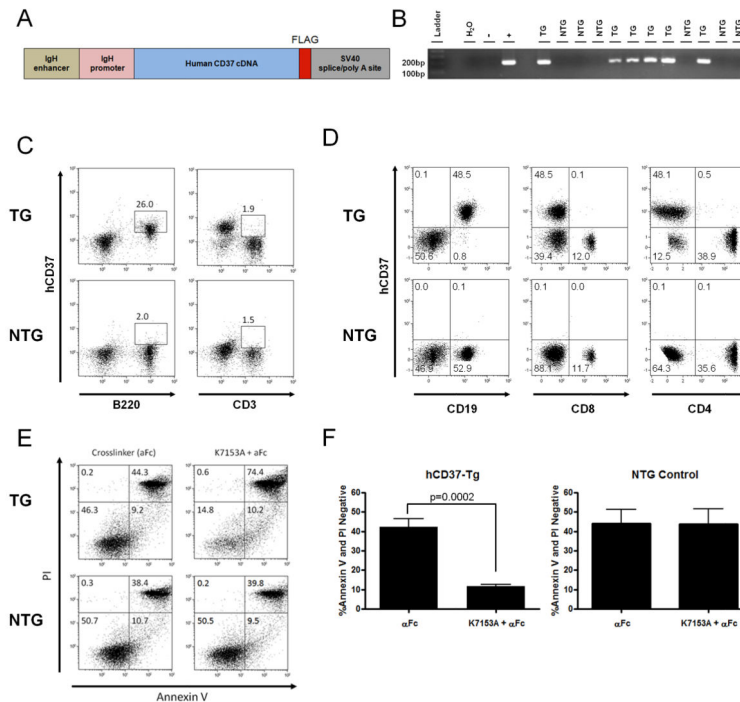


Figure 3. Generation and characterization of the human CD37 transgenic mouse
 (A) Schematic representation of the construct used to generate the hCD37-Tg mouse. (B) PCR genotyping of founder lines with human CD37 specific primers. (C) Surface expression of human CD37 on transgenic (TG; top) and non-transgenic (NTG; bottom) splenocytes. Cells stained for B220 and CD3 to analyze B and T lymphocytes, respectively. (D) Surface expression of human CD37 on transgenic (TG; top) and non-transgenic (NTG; bottom) peripheral blood leukocytes. Whole blood stained for CD19, CD4, CD8, and human CD37. After staining, RBCs were lysed and samples analyzed by flow cytometry. (E) Example of flow cytometry performed on purified splenic B-cells stained with Annexin V and propidium iodide to assess viability after 24 hour treatment with 10 μ g/ml anti-CD37 antibody (K7153A) in the presence of 50 μ g/ml goat anti-human Fc antibody (α Fc) for crosslinking. (F) Average viability of purified B-cells from transgenic or non-transgenic spleens (n=7/group) after 24 hour treatment with 10 μ g/ml anti-CD37 antibody (K7153A) in the presence of 50 μ g/ml goat anti-human Fc antibody (α Fc) for crosslinking. Mean percentage of viable cells is displayed with error bars indicating SEM.

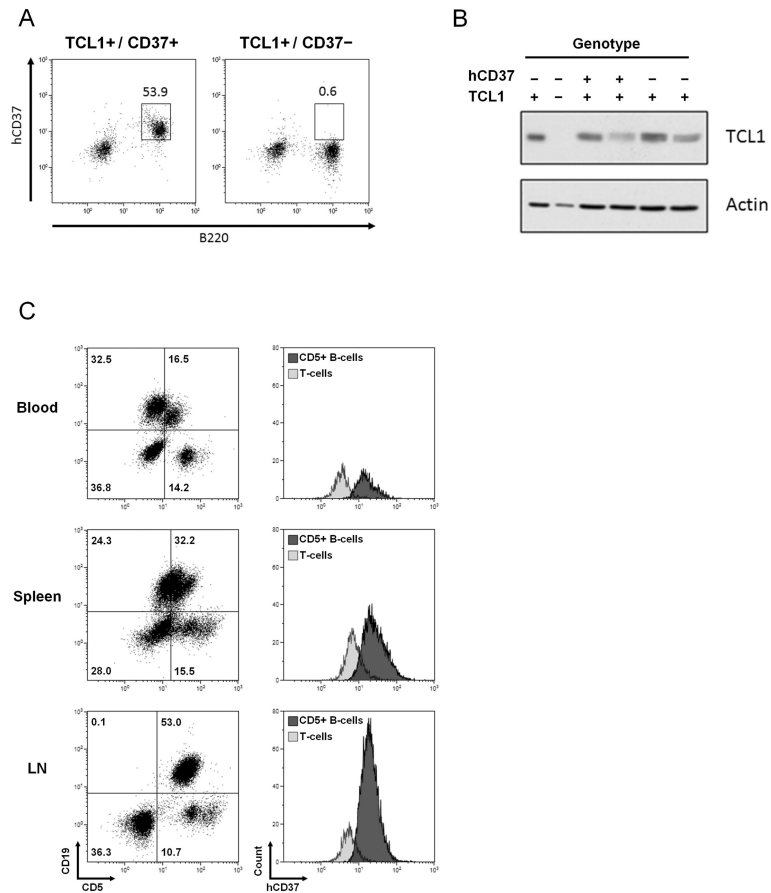


Figure 4. CD37xTCL1 double transgenic mice retain transgene expression and develop hCD37+CD19+CD5+ leukemia

(A) Flow cytometry performed on peripheral blood from a CD37xTCL1 double transgenic mouse and a TCL1 littermate. Cells were stained with antibodies against mouse B220 to label B-cells and human CD37. (B) Western blot using protein lysates from purified B-cells obtained from spleens of CD37xTCL1 mice or TCL1 littermates. Western blot is probed with anti-human TCL1 antibody. Lysates from C57BL/6 and leukemic TCL1 mice are included as controls in the first two lanes. (C) Flow cytometry performed on samples obtained from peripheral blood, spleen, and lymph nodes of a leukemic CD37xTCL1 mouse. Cells were stained for CD5, CD19, and human CD37. The right side of the panel demonstrates staining with K7153A-PE antibody and is gated on either CD5+CD19+ B-cells (dark gray histogram) or hCD37-negative T-cells (light gray histogram).

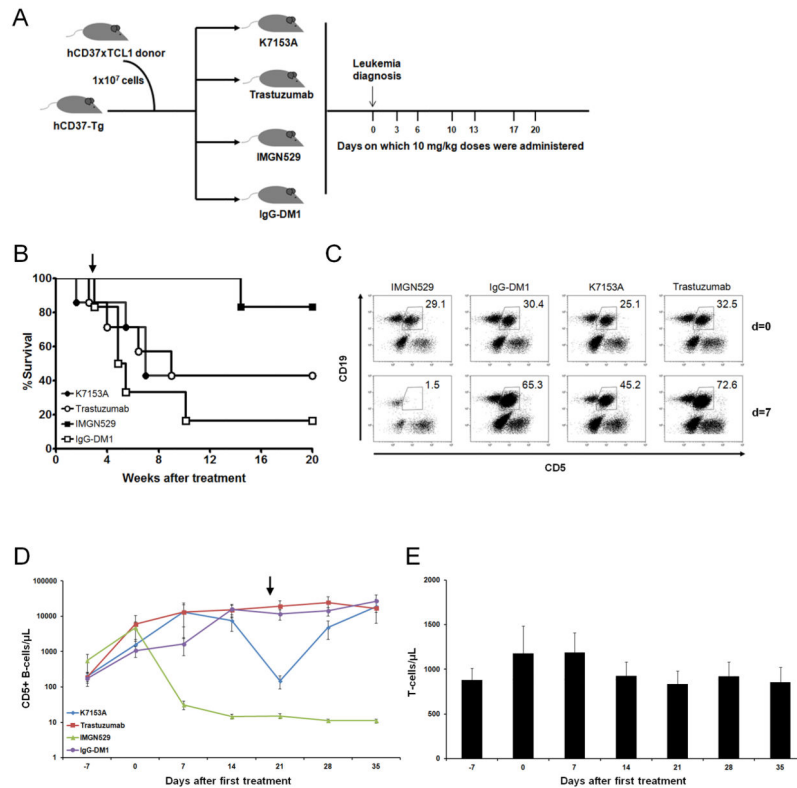


Figure 5. IMG529 demonstrates *in vivo* efficacy against hCD37+ mouse leukemia
 (A) Schematic outline of the hCD37xTCL1 engraftment experiment. Healthy hCD37-Tg recipients were injected i.v. with 1×10^7 splenocytes from a leukemic hCD37xTCL1 donor. Mice were randomly assigned (n=6-7/group) for treatment with 10 mg/kg IMG529 ADC, its K7153A antibody component, IgG-DM1 ADC control, or trastuzumab control. Treatment began following leukemia development, which was defined as when >20% of CD45+ events were CD5+CD19+ B-cells. Animals received a 10 mg/kg i.p. treatment on the day of leukemia diagnosis and repeat doses twice weekly for three weeks (70 mg/kg total). (B) Kaplan-Meier plot comparing the overall survival of engrafted mice. IMG529 significantly improved survival relative to its IgG-DM1 control (p=0.042), while parent antibody K7153A had no survival benefit compared with trastuzumab control (p=0.94). Log-rank tests were used for statistical analysis. Arrow indicates day 20, when mice received their last injection. (C) Representative examples of flow cytometry performed on mice 24h after receiving their third dose. Whole blood was stained for CD45/CD19/CD5 and plots are gated on singlet CD45+ events. (D) Absolute concentration of the CD5+CD19+ B-cell population to which the leukemia belongs. Data expressed as mean \pm SEM. Arrow indicates day 20, when mice received their last injection. (E) Concentration of T-cells in the IMG529 treated group. Mean T-cell concentration for n=6 mice is displayed with error bars indicating SEM.

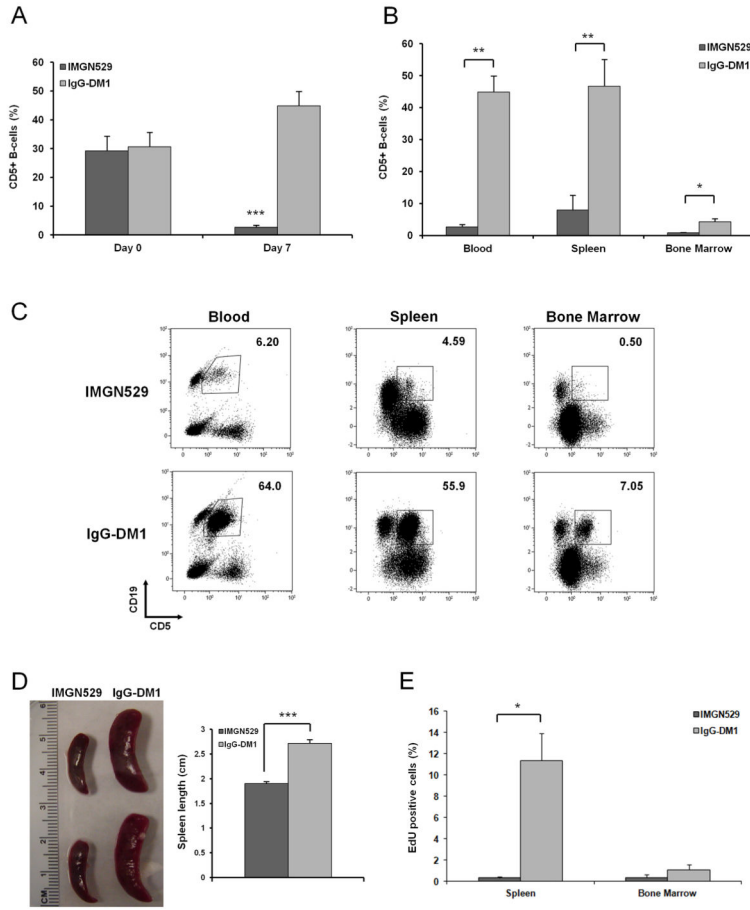


Figure 6. IMGN529 targets proliferating mouse leukemia cells within lymphoid tissues (A-E) Healthy hCD37-Tg mice engrafted with hCD37×TCL1 leukemia. Upon leukemia development (day 0), mice were randomized (n=5 mice/group) to receive 10 mg/kg i.p. doses of IMGN529 or IgG-DM1 control on days 3 and 5. To detect *in vivo* proliferation 100 µg EdU was administered on day 6 and mice were euthanized on day 7. (Mean is displayed for n=5 mice/group with error bars indicating SEM. ***p<0.0001, **p<0.01, *p<0.05) (A) Percentage CD5+CD19+ leukemia cells (of total CD45+ events) in peripheral blood on day 0 and day 7. (***p<0.0001 for change in cell percentage). (B) Percentage CD5+CD19+ leukemia cells (of total CD45+ events) in the blood, spleen, and bone marrow on day 7. (C) Examples of flow cytometry performed on peripheral blood, spleen, and bone marrow from mice treated with IMGN529 or IgG-DM1. Plots are gated on singlet, live, CD45+ cells. (D) Examples of spleens removed from mice receiving IMGN529 or IgG-DM1 (left panel) and average spleen length of all mice in the study (n=5/group; right panel). (E) Percentage of EdU+ cells among CD5+CD19+ events in the spleen and bone marrow.